

See discussions, stats, and author profiles for this publication at: <https://www.researchgate.net/publication/224975377>

Thermal and photocatalytic degradation of poly(methyl methacrylate), poly(butyl methacrylate), and their copolymers

ARTICLE

READS

33

2 AUTHORS:



N. Daraboina

University of Tulsa

36 PUBLICATIONS 406 CITATIONS

SEE PROFILE



Giridhar Madras

Indian Institute of Science

553 PUBLICATIONS 9,837 CITATIONS

SEE PROFILE

Thermal and Photocatalytic Degradation of Poly(methyl methacrylate), Poly(butyl methacrylate), and Their Copolymers

Nagu Daraboina and Giridhar Madras*

Department of Chemical engineering, Indian Institute of Science, Bangalore 560012

The photocatalytic degradation of the homopolymers, poly(methyl methacrylate) (PMMA), poly(butyl methacrylate) (PBMA), and their copolymers (PMMABMA) was studied in *o*-dichlorobenzene in the presence of commercial TiO₂ (Degussa P-25) and TiO₂ synthesized by combustion synthesis (CSN-TiO₂). Gel permeation chromatography was used to determine the evolution of molecular weight distributions with reaction time. The experimental data indicated that the polymers PMMA and PBMA and their copolymers degrade by simultaneous random and chain end scission. A continuous distribution model was developed for the mechanism involved in degradation by both random and chain end scission and used to determine the degradation rate coefficients. The degradation rate coefficients of the polymers in the presence of CSN-TiO₂ were higher than the degradation rate coefficients obtained with commercial TiO₂ (Degussa P-25). The degradation rate coefficient of copolymers was in between that of the homopolymers and increased linearly with the increase of mol % of PMMA. The degradation of PMMA, PBMA, and their copolymers was also investigated by thermogravimetric analysis. The copolymers exhibited better thermal stability than the homopolymers in contrast to that observed for photocatalytic degradation.

Introduction

Poly(alkyl methacrylate)s are well-known for their diversified applications because of their mechanical and electrical properties, optical clarity, and high chemical and thermal stability.^{1,2} Alkyl methacrylates have the ability to form copolymers with the other monomers. The properties of the polymers depend on the length of the ester side chain and the monomer ratios in the copolymer.^{3,4} Therefore, it is important to understand the properties of these polymers for industrial usage and recycling process. There are several methods used for degrading the polymers like thermal, mechanical, radiative, chemical, biological, etc. The effect of several catalysts and oxidizing agents on the polymer degradation has been extensively studied.^{5–10} The effect of alkyl group substituents on the thermal degradation of poly(alkyl methacrylate)s was studied by atom superposition and electron delocalization molecular orbital (ASED-MO) theory.¹¹ Other methods of degradation like photo-oxidative degradation,³ ultrasonic degradation,¹² and thermal degradation^{13,14} of poly(alkyl methacrylate)s have also been studied. Though the solubility and diffusivity¹⁵ of solvents in the copolymer, poly(methyl methacrylate-co-butyl methacrylate) (PMMABMA), phase behavior using interaction parameters,¹⁶ and miscibility of PMMABMA have been studied, degradation of these copolymers has not been investigated.

The fundamental studies on photodegradation of polymers are required to develop photoresists and other degradable polymers. The photodegradation of polymers is primarily photooxidative due to the presence of oxygen and results in the reduction in molecular weight and introduction of new functional groups.¹⁷ The photodegradation of poly(methyl methacrylate) (PMMA),⁹ copolymers of methyl methacrylate,⁴ and blends¹⁸ of PMMA has been studied, but the photodegradation of these polymers in solution has not been investigated. The presence of nanomaterials like titanium dioxide (TiO₂) increased the photodegradation rate of polymers.^{7,8} A new method for synthesis of titanium dioxide based on combustion

synthesis (CSN-TiO₂) has been reported,¹⁹ which has higher activity compared to that of commercial Degussa P-25 catalysts for the photodegradation of dyes, phenols, pollutants, and polymers.^{20–22} The higher activity of combustion-synthesized catalyst is due to the lower band gap and higher surface area of this catalyst compared to that of Degussa P-25.

The objective of this study was to investigate the thermal stability and photocatalytic degradation of the homopolymers and copolymers. The photocatalytic degradation of the polymers was investigated in solution (dichlorobenzene). Continuous distribution kinetics was used to determine the degradation rate coefficients. The thermal degradation of the polymers was investigated using thermogravimetry, and the study examines whether the thermal stability of the copolymers is significantly different than that of the photochemical reactivity of the copolymers.

Experimental Details

Materials. Methyl methacrylate (MMA) and *n*-butyl methacrylate (*n*-BMA) monomers were purchased from Sigma Aldrich. The monomers were purified by removing the inhibitor (hydroquinone methyl ether) by washing with 5 M NaOH solution and distilled water. The solvents, *o*-dichlorobenzene (DCB) and methanol, were purchased from SD. Fine Chemicals (India), distilled, and filtered through 0.2 μ m nylon filter paper before use. The initiator, azobisisobutyronitrile (AIBN), was purchased from SD. Fine Chemicals and purified by precipitating in acetone and recrystallization. The chemicals, *d*₂-chloroform (CDCl₃) and tetramethylsilane (TMS), used in NMR, were purchased from Sigma-Aldrich.

Polymerization. PMMA (M_{n0} = 120 000 and PD = 1.6), PBMA (M_{n0} = 112 000 and PD = 1.5), and copolymers PMMABMA-32 (32% MMA, M_{n0} = 114 000 and PD = 1.4), PMMABMA-51 (51% MMA, M_{n0} = 117 000 and PD = 1.5), and PMMABMA-69 (69% MMA, M_{n0} = 115 000 and PD = 1.4) were synthesized by solution polymerization with AIBN as the initiator at 60 °C. M_{n0} represents the initial molecular weight of the polymer, and PD represents the polydispersity of the

* To whom correspondence should be addressed. Tel.: 091-80-22932321. Fax: 091-80-23600683. E-mail: giridhar@chemeng.iisc.ernet.in.

polymer. These were determined by gel permeation chromatography. Predetermined quantities of MMA, BMA, DCB, and AIBN were placed in polymerization tubes, and the mixture was flushed with N₂ for 15 min. These tubes were tightly sealed and immersed in a visual thermostatted water bath, heated by means of a PID controller (Techno Scientific, India) that maintained the temperature at 60 ± 1 °C. After the reaction, the copolymers were precipitated in methanol and dried at 50 °C.

Characterization. The copolymer compositions were determined by ¹H NMR (400 MHz, Bruker) spectroscopy at room temperature with CDCl₃ as solvent and TMS as the internal standard. The NMR spectra for the copolymers with different MMA compositions are shown in Figures S1a–S1c (see Supporting Information). The methyl methacrylate monomer has a singlet peak at δ = 3.8 ppm. This peak corresponds to the methoxy of the ester linkage. Similarly, the butyl methacrylate monomer shows a triplet peak at δ = 4.2 ppm. This peak corresponds to the ethyleneoxy of the ester linkage.^{4,23,24} These two peaks are identified in all copolymers. The respective monomer compositions of the copolymers were determined from the integrated peak areas.⁴ The peak intensity at δ = 3.8 ppm increases with increase in MMA content (Figures S1a, S1b, S1c).

Synthesis and Characterization of Nano TiO₂. The solution combustion method was used for the preparation of anatase CSN-TiO₂ by using titanyl nitrate as precursor with oxalyldihydrazide as fuel. Oxalyldihydrazide (ODH) was prepared from diethyl oxalate (Merck Chemicals, India) and hydrazine hydrate (Merck Chemicals). Titanyl nitrate was synthesized by reacting titanyl hydroxide obtained by the hydrolysis of titanium isopropoxide (Lancaster Chemicals, UK) with nitric acid. The solution combustion synthesis involves the combustion of aqueous solutions containing stoichiometric amounts of titanyl nitrate and ODH. A pyrex dish (300 mL) containing an aqueous redox mixture of stoichiometric amounts of titanyl nitrate and ODH in 30 mL of water was introduced into the muffle furnace, which was preheated to 350 °C. The solution initially undergoes dehydration, and a spark appearing at one corner spreads throughout the mass and yields anatase phase TiO₂. Further details of preparation are given elsewhere.^{25,26} The catalyst was characterized using X-ray diffraction, BET surface area, TGA/DTA, UV, and IR spectrometer.²⁵ The catalyst is nanosized and crystalline. The catalyst has a lower band gap of 2.65 eV and a higher surface area (156 m²/g) than that of commercial Degussa P-25, whose band gap is 3.1 eV and surface area is 50 m²/g. The catalyst has more surface hydroxyl groups, as evidenced by FTIR analysis and TGA/DTA.²⁵

Photochemical Reactor. A high-pressure mercury vapor lamp of 125 W (Samson lamps) was used as the light source by removing the outer cover. The lamp was connected in series with a ballast and capacitor to minimize the fluctuation in the input supply. It was placed in a jacketed quartz tube (for cooling by water circulation) of 3.4 cm inner diameter, 4 cm outer diameter, and 21 cm length to maintain the constant temperature. The reaction vessel was a glass cylinder of 6 cm inner diameter and 16 cm height. The polymer sample solution was stirred with a magnetic stirrer and was placed 3 cm above the stirrer. Further details of the photochemical reactor are provided elsewhere.^{25,26} The lamp emitted predominantly at 365 nm, and the photon flux was 5 × 10⁻⁶ mol of photon/s.

Degradation Experiments. An amount of 90 mL of polymer solution of concentration 2 g/L in dichlorobenzene was taken each time, and the concentration of catalyst was fixed at 1 g/L

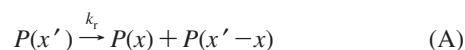
for all the experiments to study the degradation kinetics. Samples of solutions were collected at different time intervals for GPC analysis. The samples were centrifuged and filtered before GPC analysis to remove the catalyst particles. Multiple experiments indicated that the error in rate coefficient was approximately 2%.

Gel Permeation Chromatography Analysis. The samples were analyzed in gel permeation chromatography. The system consists of a high-pressure liquid chromatography (HPLC) pump (Waters 515) for pumping the eluent, THF at a flow rate of 1 mL/min, Rheodyne 7725i injector, and three size exclusion columns packed with cross-linked poly(styrene-divinyl benzene) (Styragel HR-5E, HR 4, HR 1) maintained at 50 °C. A differential refractive index detector (Waters RI 2410) was used for detection and stored using a data acquisition system. Calibration was carried out with polystyrene standards.

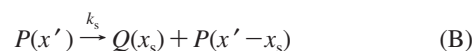
Thermogravimetric Analysis. An amount of 10–15 mg of polymer was pyrolyzed in an inert atmosphere with a flow of nitrogen at 150 cm³/min in a thermogravimetric analyzer (TGA) (Perkin-Elmer, Pyris). The temperature was raised from 25 to 750 °C at heating rates of 5 and 10 °C/min.

Differential Scanning Analysis. The glass transition temperatures of various blends were recorded in a differential scanning calorimeter (DSC, Perkin-Elmer). The experiments were carried out in an inert atmosphere (N₂) from -100 to 200 °C in an aluminum pan with a heating rate of 2 °C/min. The glass transition temperatures were determined by differentiating the DSC signal.

Theoretical Model. Continuous distribution kinetics was used to study the degradation kinetics of the polymers PMMA and PBMA and copolymers. The following reactions represent the polymer degradation by combined random chain scission



and specific chain end scission



$P(x)$ represents the polymer of molecular weight x , and $p(x, t)$ represents the instantaneous molar molecular weight distribution (MWD) of the polymer. $Q(x_s)$ represents a specific product with molecular weight x_s in chain end scission, and $q(x, t)$ represents the MWD of the specific product. For reactions (A) and (B), the random chain scission and specific chain scission rate coefficients are k_r and k_s , respectively. The population balance equations for the above reactions are

$$\frac{\partial p(x, t)}{\partial t} = -k_r(x)p(x, t) + 2 \int_x^\infty k_r(x')p(x', t)\Omega(x, x')dx' - k_s(x)p(x, t) + \int_x^\infty k_s(x')p(x', t)\Omega(x - x_s, x')dx' \quad (1)$$

$$\frac{\partial q(x, t)}{\partial t} = \int_x^\infty k_s(x')p(x', t)\Omega(x_s, x')dx' \quad (2)$$

For random chain scission, the distribution of degraded products is given by the stoichiometric kernel²⁷ $\Omega(x, x')$, and $1/x'$. For chain end scission, the stoichiometric kernels^{27,28} are represented by Dirac delta functions, $\Omega(x - x_s, x') = \delta(x - x' + x_s)$ and $\Omega(x, x') = \delta(x - x_s)$, for products having molecular weights $x - x_s$ and x_s , respectively. Assuming that the degradation rate coefficient for random scission is linearly dependent on the molecular weight of the polymer,²⁹ i.e., $k_r(x) = k_r x$, the degradation rate coefficient for specific chain scission

is independent of molecular weight.²⁷ Applying the moment operation, $p^{(j)}(t) = \int_0^\infty p(x,t)x^j dx$, to eqs 1 and 2 yields

$$\frac{dp^{(j)}}{dt} = -\left(\frac{j-1}{j+1}\right)k_p p^{(j+1)} - k_s p^{(j)} + k_s \sum_{i=0}^j j c_i p^{(j-i)} (-x_s)^j \quad (3)$$

$$\frac{dq^{(j)}}{dt} = k_s x_s^{(j)} p^{(0)}(t) \quad (4)$$

The initial conditions for the equations are $p^{(j)}(t=0) = p_0^{(j)}$ and $q^{(j)}(t=0) = 0$. $j=0$ and 1 correspond to the zeroth and first moments, respectively. $p^{(0)}$ is the molar concentration of the polymer (mol/L), and $p^{(1)}$ is the mass concentration of the polymer (g/L).

$$\frac{dp^{(0)}}{dt} = k_p p^{(1)} \quad (5)$$

$$\frac{dp^{(1)}}{dt} = -k_s x_s p^{(0)} \quad (6)$$

$$\frac{dq^{(1)}}{dt} = k_s x_s p^{(0)} \quad (7)$$

The initial conditions for the above equations are $p^{(0)}(t=0) = p_0^{(0)}$, $p^{(1)}(t=0) = p_0^{(1)}$, and $q^{(1)}(t=0) = 0$.

From eqs 6 and 7, $(dp^{(1)}/dt) + (dq^{(1)}/dt) = 0$; i.e., the rate of change of mass concentration is zero. Solving the simultaneous eqs 5 and 6 with the given initial conditions gives

$$p^{(0)} = p_0^{(0)} \cos(kt) + p_0^{(1)} \left(\frac{k_r}{k}\right) \sin(kt) \quad (8)$$

$$p^{(1)} = p_0^{(1)} \cos(kt) - p_0^{(0)} \left(\frac{k}{k_r}\right) \sin(kt) \quad (9)$$

where $k = \sqrt{k_r k_s x_s}$.

The number average molecular weight is defined as $M_n = p^{(1)}/p^{(0)}$. Thus, from eqs 8 and 9

$$M_n = \frac{kk_r M_{no} - k^2 \tan(kt)}{kk_r + k_r^2 M_{no} \tan(kt)} \quad (10)$$

Results and Discussion

The reactivity ratios of the monomers were determined by the Fineman–Ross method³⁰ based on the polymer composition determined by NMR. The reactivity ratios for MMA and BMA (r_1 and r_2) were 0.71 and 0.82, respectively. The reactivity ratios are consistent with the published data⁴ in that $r_1 < r_2$ and $r_1 r_2 < 1$. Because of the latter condition, the resulting copolymers are random, consistent with earlier studies.^{4,32}

The glass transition temperatures (T_g) of the copolymers were determined by differential scanning calorimetry (DSC). The DSC measurements showed single, narrow transitions confirming the randomness of the copolymer. The glass transition temperatures of the copolymers were in between the T_g of the respective homopolymers. Figure 3 shows the T_g of the copolymers with the increasing wt % of the MMA. The T_g can be predicted by the Fox equation⁴ (eq 11) or the modified Gordon–Taylor equation (eq 12)

$$\frac{1}{T_g} = \frac{w_{mma}}{T_{gmma}} + \frac{w_{bma}}{T_{gbma}} \quad (11)$$

$$T_g = w_{mma} T_{gmma} + w_{bma} T_{gbma} \quad (12)$$

where w_{mma} and w_{bma} are the weight fractions of each monomer in the copolymer and T_{gmma} and T_{gbma} are the glass transition temperatures of PMMA and PBMA, respectively.

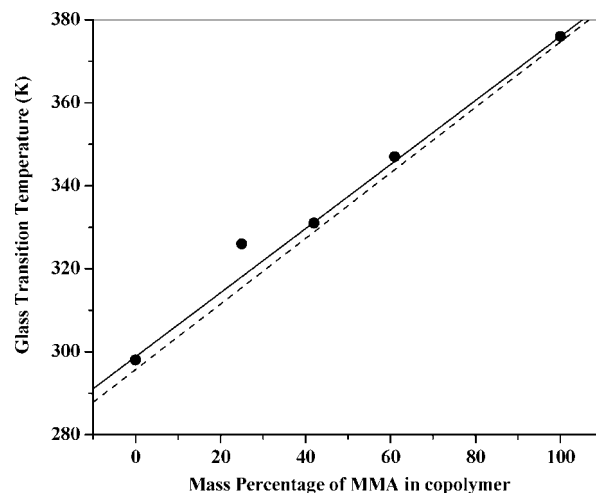


Figure 1. Comparison of experimental T_g of copolymers with Fox prediction. Legend: experimental (●), Fox prediction (---), and Gordon–Taylor (—).

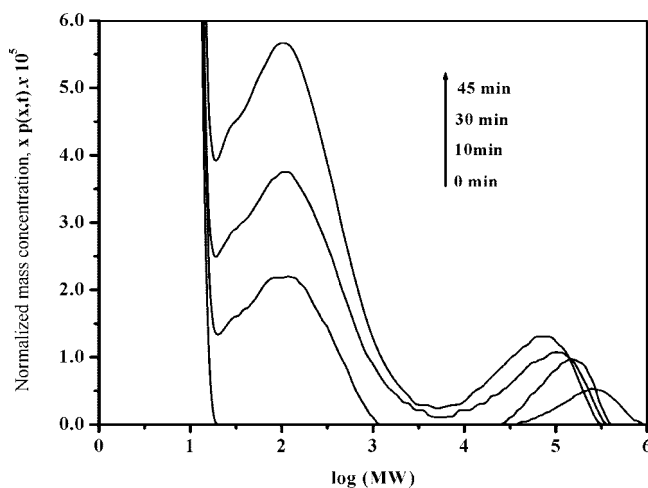


Figure 2. Evolution of the normalized mass distribution of the copolymer (69 mol % MMA) with reaction (photodegradation) time.

However, Figure 1 shows that the experimental values are slightly different from the prediction of the Fox and Gordon–Taylor equations, which may be attributed to strong specific interactions like dipole–dipole interactions. A similar observation was reported for different compositions of these copolymers.⁴

The degradation of the homopolymers, PMMA and PBMA, and the copolymers of MMA and BMA was studied with UV in the absence and in the presence of two catalysts (P-25 and CSN–TiO₂). Both random and chain end scission were observed in the photocatalytic degradation of these polymers. The experimental MWD (Figure 2) shows a shift in the main polymer peak due to the random scission and the formation of a second peak. This second peak represents the formation of a specific product of molecular weight 400 due to the chain end scission. Figures 3a–e show the variation of number average molecular weight with time for the homopolymers and copolymers. The rate coefficients of both random and chain end scission of these polymers were obtained by fitting the model with the experimental data and are given in Table 1.

The values of the degradation rate coefficients obtained from the model indicated that the degradation of the polymer by random scission enhanced nearly 1.2 to 1.5 times in presence of Degussa P-25 and 1.8 to 2.7 times in presence of CSN–TiO₂

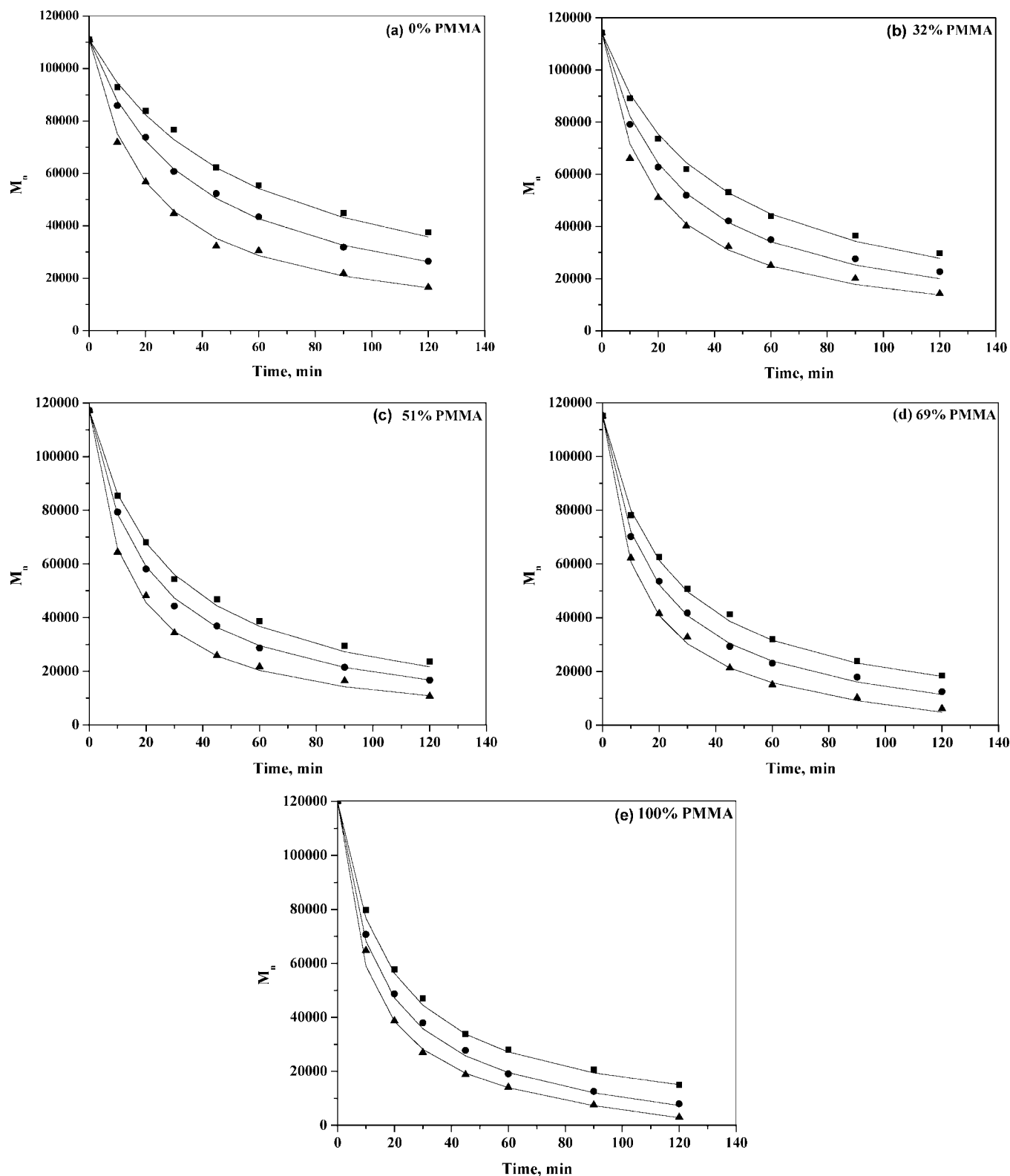


Figure 3. Variation of the number average molecular weight of copolymer as a function of time for (a) 0 mol % MMA (PBMA), (b) 32 mol% MMA, (c) 51 mol % MMA, (d) 69 mol % MMA, and (e) 100 mol % MMA (PMMA). Legend: (■) UV without catalyst, (●) UV + P-25, and (▲) UV + CSN-TiO₂. Solid lines are model fit.

compared to the noncatalytic process. In case of specific chain end scission, the rate coefficient is enhanced by 1.3 to 1.7 times in presence of P-25 and 1.6 to 2.4 times in presence of CSN-TiO₂ compared to the noncatalytic process. The degradation rate coefficient for both random and specific chain end scission increases linearly with the increase in % of PMMA in the copolymer, as shown in Figure 4. It has been shown that³

PMMA, on UV exposure, undergoes faster degradation and depolymerization but slower oxidation and destruction of ester group than PBMA. Thus, in a random copolymer of MMA and BMA, the rate of photodegradation increases linearly with increasing MMA composition in the copolymer.

Photodegradation is mainly photooxidative where the chain scission is triggered by hydrogen abstraction from the main chain

Table 1. Rate Constants Obtained by Fitting the Model with Experimental Data

polymer	UV		UV + P-25		UV + CSN-TiO ₂	
	$k_r \times 10^8$ (mol g ⁻¹ min ⁻¹)	$k_s \times 10^3$ (min ⁻¹)	$k_r \times 10^8$ (mol g ⁻¹ min ⁻¹)	$k_s \times 10^3$ (min ⁻¹)	$k_r \times 10^8$ (mol g ⁻¹ min ⁻¹)	$k_s \times 10^3$ (min ⁻¹)
PMMABMA-0	15.6	3.20	24.3	4.10	43.4	6.60
PMMABMA-32	22.5	7.10	34.6	8.40	56.2	12.4
PMMABMA-51	31.8	9.30	42.1	11.4	67.1	17.1
PMMABMA-69	38.8	11.8	51.2	15.6	75.9	21.3
PMMABMA-100	47.1	17.1	67.8	21.7	82.7	27.6

by a hydroxyl radical or reaction with oxygen to form peroxide radicals. It was determined that only 1% of the hydroxyl radicals formed are involved directly in main chain scission, whereas the remaining participate in hydrogen abstraction and other radical reactions for irradiation by high-energy rays.³¹ The enhanced degradation by CSN-TiO₂ is mainly due to the presence of large number of hydroxyl groups on its surface that help in the generation of many macroradicals. CSN-TiO₂ possesses nearly 10 times the number of hydroxyl groups²⁶ on its surface than that in Degussa P-25. The reduced band gap and high surface area are also important factors in enhancing catalyst activity.

To examine whether this trend is observed for other modes of degradation, thermal degradation of PMMA, PBMA, and copolymers was studied at different heating rates of 5 °C/min and 10 °C/min in TGA (thermogravimetric analysis) under

nitrogen flow. Figure 5 shows the normalized weight loss profiles for the degradation of polymers at 5 and 10 °C/min. The weight loss profiles of homopolymers were comparable with the previous studies.^{14,33} The degradation of homopolymers started at 220 °C and continued until 400 °C. However, the degradation of the copolymers started at 150 °C and ended at 450 °C. PMMABMA-52 and PMMABMA-69 showed degradation in two stages. The first stage is in between 180 and 310 °C and the second stage is between 310 and 450 °C. The two-stage degradation was also observed in allyl methacrylate copolymers with methyl methacrylate.³⁴ The temperatures at different conversions for both homopolymers and copolymers are shown in Figure 6. The numbers in Figure 6 represent the fraction of the polymer that has degraded. The copolymers have lower thermal stability than PMMA and PBMA for <15% degradation. However, the copolymers showed better thermal

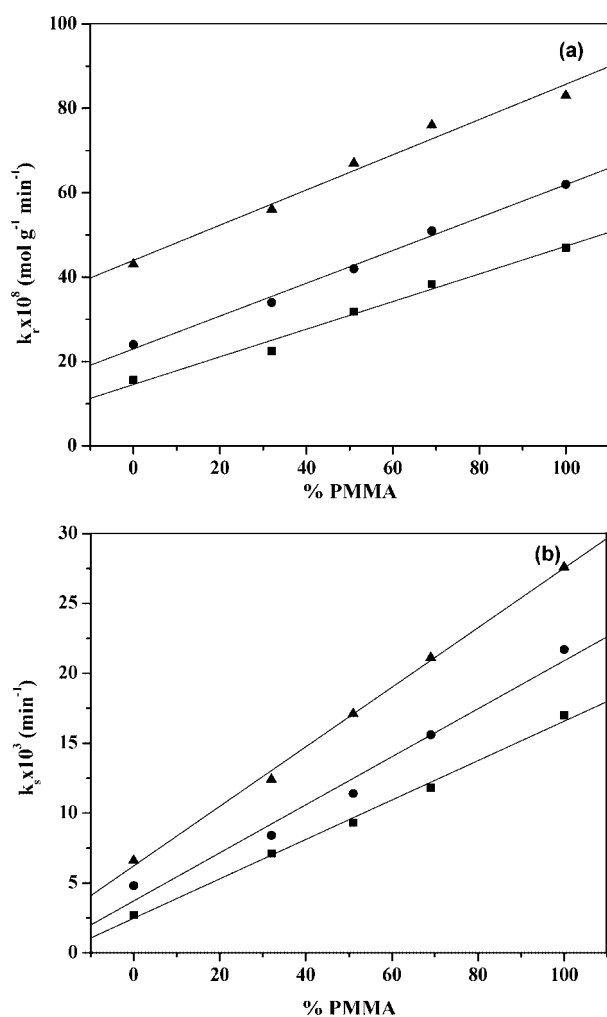


Figure 4. Variation of degradation rate coefficient with the mol % of MMA in copolymer. (a) Random chain scission. (b) Specific chain end scission. Legend: (■) UV without catalyst; (●) UV + P-25; and (▲) UV + CSN-TiO₂. Solid lines are model fit.

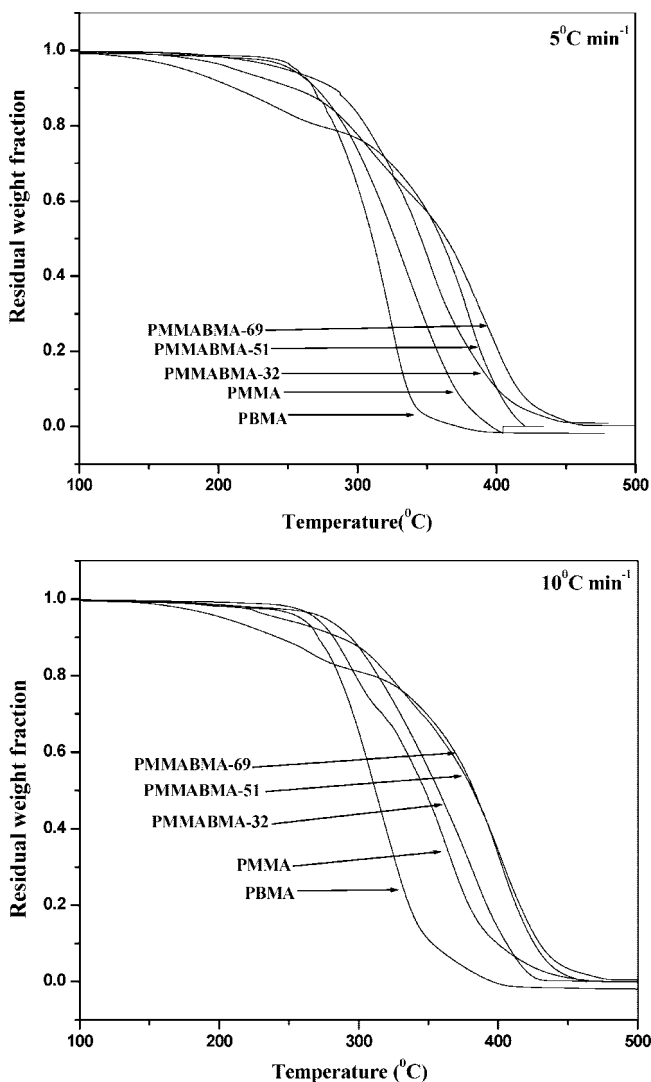


Figure 5. Thermogravimetric profiles for MMA-BMA homopolymers and copolymers with heating rates of (a) 5 °C/min and (b) 10 °C/min.

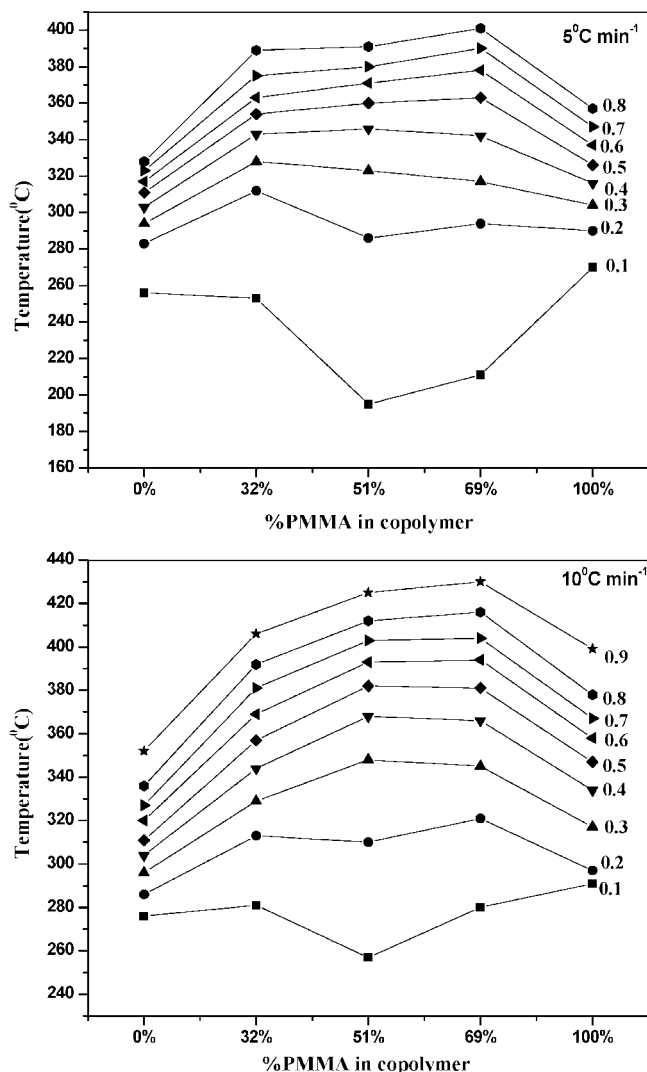


Figure 6. Variation of degradation temperature with % MMA in the copolymers at various conversions with heating rates of (a) 5 °C/min and (b) 10 °C/min. The numbers on the figure represent the conversion, i.e., fraction of the polymer that has degraded.

stability than the homopolymers PMMA and PBMA at higher conversions. Irrespective of the heating rate, the stability of the copolymers is higher than that of the homopolymers for >20% conversions. Similar trends were observed in the copolymers of allyl methacrylate and methyl methacrylate,³⁴ where it was observed that if the degree of degradation was higher than 40% then the copolymers were more stable and show slower subsequent weight loss compared to the homopolymers.

All poly(alkyl methacrylates) yield monomer as the predominant volatile product of thermal degradation. It has been proposed that monomer formation at lower temperature is due to initiation at unsaturated chain ends. However, degradation at higher temperature is associated with the initiation of random scission. The initiation of this random process may be slow with an increase in MMA content in copolymers. Thus, the copolymers are more thermally stable than the homopolymers at high conversions.

Thus, the thermal stability of the copolymer varies with the degree of decomposition, but the stability of the copolymers during photocatalytic degradation follows the linear relationship with the mol % of MMA in the copolymers.

Conclusions

The copolymers of various compositions of MMA/BMA were synthesized by solution polymerization technique and character-

ized by ¹H NMR spectroscopy. Fineman–Ross plot and the DSC analysis indicated that random copolymers were formed. The photodegradation of these copolymers was determined in the absence of catalyst and in the presence of two different catalysts. Simultaneous random and chain end scission was observed in all cases for all polymers. A model based on continuous distribution kinetics was developed considering both random and chain end scission. The degradation rate coefficients were determined by fitting the model to experimental data. The photocatalytic degradation rate coefficient of the copolymers increased linearly with the increase in MMA composition for both random and chain end scission. However, the thermal stability of the copolymers depends on the degree of degradation with the copolymers being more stable than the homopolymers at higher conversions.

Acknowledgment

The corresponding author acknowledges the Department of Science and Technology, India, for financial support and the Swarnajayanti Fellowship.

Supporting Information Available: Figure S1 shows the NMR spectrum trace for MMA/BMA copolymers containing (a) 32 mol %, (b) 51 mol %, and (c) 69 mol % of MMA. This material is available free of charge via the Internet at <http://pubs.acs.org>.

Literature Cited

- (1) Mark, H. F.; Bikales, N. M.; Overberger, Ch. G.; Menges, G.; Kroschwitz, J.I., Eds.; *Encyclopedia of polymer science and engineering*; Wiley Interscience: NY, 1985; Vol. 1, p 234.
- (2) Bandrup, J.; Immergut, E. H. *Polymer Handbook*, 2nd ed.; Wiley Interscience: NY, 1975.
- (3) Kaczmarek, H.; Kaminska, A.; Herk, A. V. Photo oxidative degradation of poly(alkyl methacrylate)s. *Eur. Polym. J.* **2000**, *36*, 767.
- (4) Vail, N. K.; Barlow, J. W.; Beaman, J. J.; Marcus, H. L.; Bourell, D. L. Development of a poly (methyl methacrylate-co-n-butyl methacrylate) copolymer binder system. *J. Appl. Polym. Sci.* **1994**, *52*, 789.
- (5) Hideki, S.; Masako, N. Thermal decomposition of additive polymerization initiators. I. Azo-bisisobutyronitrile. *J. Appl. Polym. Sci.* **1967**, *11*, 2097.
- (6) Gupte, S.; Madras, G. Catalytic degradation of polybutadiene. *Polym. Degrad. Stab.* **2004**, *86*, 529.
- (7) Sivalingam, G.; Madras, G. Photocatalytic degradation of poly-(bisphenol-A-carbonate) in solution over combustion-synthesized TiO₂: mechanism and kinetics. *Appl. Catal. A: Gen.* **2004**, *269*, 81.
- (8) Vijayalakshmi, S. P.; Madras, G. Photocatalytic degradation of poly (ethylene oxide) and poly acrylamide. *J. Appl. Polym. Sci.* **2006**, *100*, 3997.
- (9) Allison, J. P. Photodegradation of poly(methyl methacrylate). *J. Polym. Sci.* **1966**, *4*, 1209.
- (10) Chiantore, O.; Trossarelli, L.; Lazzari, M. Photooxidative degradation of acrylic and methacrylic polymers. *Polymer* **2000**, *41*, 1657.
- (11) Awad, M. K. Effect of alkyl substituents on the thermal degradation of poly (alkyl methacrylate): a molecular orbital study using the ASEDMO method. *Polym. Degrad. Stab.* **1995**, *49*, 339.
- (12) Malhotra, S. L. Ultrasonic solution degradations of poly (alkyl methacrylates). *J. Macromol. Sci. Chem.* **1986**, *23*, 729.
- (13) Song, J.; Fischer, Ch. H.; Schnabel, W. thermal oxidative degradation of poly (methyl methacrylate). *Polym. Degrad. Stab.* **1992**, *36*, 261.
- (14) Marimuthu, A.; Madras, G. Effect of alkyl group substituents on the degradation of poly (alkyl methacrylates) in supercritical fluids. *Ind. Eng. Chem. Res.* **2007**, *46*, 15.
- (15) Eser, H.; Tihminlioglu, F. Solubility and diffusivity of solvents and nonsolvents in poly (methyl methacrylate co butyl methacrylate). *Fluid Phase Equilib.* **2005**, *237*, 68.
- (16) Kammer, H. W.; Piglowski, J. Miscibility studies of poly (methyl methacrylate-co-butyl methacrylate) with poly (styrene-co-acrylonitrile): Phase behaviour and interaction parameters. *Acta Polym.* **1989**, *40*, 363.
- (17) Schnabel, W. J. Oxidative degradation processes in synthetic and biological polymers as studied by pulse radiolysis experiments. *Radioanal. Nucl. Chem.* **1986**, *101*, 413.

- (18) Guerrero, A. R.; Ramirez, J. C. Photodegradation of poly (methacrylate)/bisphenol A polycarbonate blends. *Polym. Bull.* **1994**, *33*, 541.
- (19) Nagaveni, K.; Hegde, M. S.; Ravishankar, N.; Madras, G. Synthesis and structure of nanocrystalline TiO₂ with lower band gap showing high photocatalytic activity. *Langmuir* **2004**, *20*, 2900.
- (20) Gupta, S. L.; Agarwal, N.; Madras, G.; Nagaveni, K.; Hegde, M. S. Effect of aluminium chloride and Pt/TiO₂ on the thermal degradation of poly(vinyl chloride) in solution. *J. Appl. Polym. Sci.* **2003**, *90*, 3532.
- (21) Priya, M. H.; Madras, G. Kinetics of photocatalytic degradation of chlorophenol, nitrophenol and their mixtures. *Ind. Eng. Chem. Res.* **2006**, *45*, 482.
- (22) Priya, M. H.; Madras, G. Photocatalytic degradation of nitrobenzenes with combustion synthesized nano-TiO₂. *J. Photochem. Photobiol. A: Chem.* **2006**, *178*, 1.
- (23) Bovey, F. A. *Nuclear magnetic resonance spectroscopy*, 2nd ed.; Academic Press: San Diego, 1988.
- (24) Pouchert, C. J. *The Aldrich library of NMR spectra*; 2nd ed.; Aldrich Chemicals: Milwaukee, 1983.
- (25) Nagaveni, K.; Sivalingam, G.; Hegde, M. S.; Madras, G. Solar photocatalytic degradation of dyes: high activity of combustion synthesized nano TiO₂. *Appl. Catal., B* **2004**, *48*, 83.
- (26) Sivalingam, G.; Nagaveni, K.; Hegde, M. S.; Madras, G. Photocatalytic degradation of various dyes by combustion synthesized nano anatase TiO₂. *Appl. Catal., B* **2003**, *45*, 23.
- (27) Koda, Y.; McCoy, B. J. Distribution kinetics of radical mechanisms: reversible polymer decomposition. *AIChE J.* **1997**, *43*, 3205.
- (28) Madras, G.; McCoy, B. J. Time evolution to similarity solutions for polymer degradation. *AIChE J.* **1998**, *44*, 647.
- (29) Madras, G.; Chung, G. Y.; Smith, J. M.; McCoy, B. J. Molecular weight effect on the dynamics of polystyrene degradation. *Ind. Eng. Chem. Res.* **1997**, *36*, 2019.
- (30) Fineman, M.; Ross, S. D. Linear method to determining monomer reactivity ratios in copolymerization. *J. Polym. Sci.* **1950**, *5*, 259.
- (31) Grollmann, U.; Schnabel, W. Free radical-induced oxidative degradation of polyacrylamide in aqueous solution. *Polym. Degrad. Stab.* **1982**, *4*, 203.
- (32) Munk, P. *Introduction to Macromolecular Science*; Wiley: New York, 1989.
- (33) Kang, B. S.; Kim, S. G.; Kim, J. S. Thermal degradation of poly(methyl methacrylate) polymers: Kinetics and recovery of monomers using a fluidized bed reactor. *J. Anal. Appl. Pyrolysis* **2008**, *81*, 7.
- (34) Zulfigar, S.; Masud, K.; Piracha, A.; McNeill, I. C. Thermal degradation of allyl methacrylate-methyl methacrylate copolymers. *Polym. Degrad. Stab.* **1997**, *55*, 257.

Received for review June 4, 2008

Revised manuscript received July 23, 2008

Accepted July 23, 2008

IE800883N